

Evaporation loss along the Calueque-Oshakati Canal in the Cuvelai-Etoshia Basin (Northern Namibia): evidence from stable isotopes and hydrochemistry

Paul Koeniger , Josefina Hamutoko , Vincent E. A. Post , Matthias Beyer , Marcel Gaj , Thomas Himmelsbach & Heike Wanke

To cite this article: Paul Koeniger , Josefina Hamutoko , Vincent E. A. Post , Matthias Beyer , Marcel Gaj , Thomas Himmelsbach & Heike Wanke (2020): Evaporation loss along the Calueque-Oshakati Canal in the Cuvelai-Etoshia Basin (Northern Namibia): evidence from stable isotopes and hydrochemistry, *Isotopes in Environmental and Health Studies*, DOI: [10.1080/10256016.2020.1830082](https://doi.org/10.1080/10256016.2020.1830082)

To link to this article: <https://doi.org/10.1080/10256016.2020.1830082>



© 2020 The Author(s). Published by Informa UK Limited, trading as Taylor & Francis Group



[View supplementary material](#)



Published online: 22 Oct 2020.



[Submit your article to this journal](#)



Article views: 145




[View related articles](#)



[View Crossmark data](#)

Evaporation loss along the Calueque-Oshakati Canal in the Cuvelai-Etoshia Basin (Northern Namibia): evidence from stable isotopes and hydrochemistry

Paul Koeniger ^a, Josefina Hamutoko^b, Vincent E. A. Post^a, Matthias Beyer^c, Marcel Gaj^d, Thomas Himmelsbach^a and Heike Wanke^e

^aFederal Institute for Geosciences and Natural Resources (BGR), Hannover, Germany; ^bGeology Department, University of Namibia (UNAM), Windhoek, Namibia; ^cUmweltgeochemie (IGOE), Technical University, Braunschweig, Germany; ^dGlobal Institute for Water Security (GIWS), Saskatoon, Canada; ^eDepartment Geography and Environmental Management, University of the West of England, Bristol, UK

ABSTRACT

Since 1973, Kunene River water has been carried from the Calueque reservoir in Angola along a 160 km open concrete canal to the town of Oshakati in the central part of the Cuvelai-Etoshia Basin and has been supplying drinking water to the most densely populated rural area of Namibia. Despite its importance for the region, intra-seasonal water quality and the technical condition of the canal are not routinely checked. Water samples were collected during four field campaigns right before the onset of the rainy season (November 2013 and 2014), and after the rainy season (June 2014 and May 2015), at 16 sites along the canal for stable water isotopes (deuterium, oxygen-17 and oxygen-18) and hydrochemical analyses. The isotope patterns and chemical composition of the canal water is discussed in comparison to local rain, Kunene source water, surface water and groundwater. Clear isotope enrichment indicates evaporative loss of water. A Craig-Gordon model was used to estimate water loss. The loss increases with distance from the source with a maximum of up to 10 %, depending on the season. The results are discussed in context of water availability, vulnerability and water resources management in this water-scarce area.

ARTICLE HISTORY

Received 24 February 2020
Accepted 6 September 2020


KEYWORDS

Cuvelai-Etoshia Basin; evaporation loss; hydrochemistry; hydrogen-2; isotope hydrology; Namibia; oxygen-17; oxygen-18; water

1. Introduction

In densely populated arid and semi-arid regions, water authorities often face severe problems to provide enough water of sufficient quality. Hydrochemical studies combined with stable isotope methods can enable a better understanding of the dominant hydrological processes, which can support water management. Stable isotope (^2H , ^{17}O and ^{18}O) signatures in water are influenced by phase transition processes in the water cycle (e.g. evaporation, condensation, sublimation, etc.). Monitoring of stable isotope variability

CONTACT Paul Koeniger  paul.koeniger@bgr.de

 Supplemental data for this article can be accessed at <https://doi.org/10.1080/10256016.2020.1830082>.

© 2020 The Author(s). Published by Informa UK Limited, trading as Taylor & Francis Group
This is an Open Access article distributed under the terms of the Creative Commons Attribution-NonCommercial-NoDerivatives License (<http://creativecommons.org/licenses/by-nc-nd/4.0/>), which permits non-commercial re-use, distribution, and reproduction in any medium, provided the original work is properly cited, and is not altered, transformed, or built upon in any way.

allows investigating water balance components such as groundwater recharge, groundwater contribution to rivers, mixing of tributaries, as well as evaporation loss from soils and surface water [1–3].

Many studies on rivers and surface waters using stable isotopes have provided useful information on hydrological processes, especially following the establishment of the Global Network of Isotopes in Rivers (GNIR), which was initiated by the IAEA [4–8]. River water isotopic compositions directly reflect contributions from headwaters and tributary rivers in a catchment [4–8]. In natural river systems, it is possible to quantify river water components, such as pre-event and event water or base-flow and direct flow components [5].

During evaporation, the water molecules containing heavier isotopes get progressively enriched in the liquid phase, due to their higher vapour pressure and lower kinetic energy. The Craig and Gordon model, which was already published in the early 1960s [1], was the first comprehensive quantitative framework for the evaporative enrichment of heavier isotopes in natural waters. Since this work, many studies have successfully used this model to estimate evaporation from lakes and surface water [2,3], as well as transpiration from soil and plant systems [9]. Considering that novel instrumental developments are now providing higher accuracies and time resolution, new perspectives and application possibilities are emerging. For example, Surma et al. [10] recently demonstrated the usefulness of ^{17}O to study recharge and evaporation processes in salt lakes in the Chilean Atacama Desert.

This study focuses on Northern Namibia, where socio-cultural and economic aspects have a large impact on water resources management practices [11–14]. Problems include, amongst others, loss of traditional knowledge on water usage caused when providing external water sources, population increase, frequent flooding and droughts. Rising population numbers in the already relatively densely populated area, and drought index classification after [13], indicate a rising water demand. Since 1973, Kunene River water has been carried from the Calueque reservoir in Angola along a 160-km concrete canal to the city of Oshakati in the central part of the Cuvelai Etosha Basin (CEB). The canal supplies between 47 million and 63 million m^3 drinking water per year [15–17]. Water losses and water quality deterioration form the main threats to a safe and sustainable water supply. Covering the canal would reduce evaporation loss but also foster social tensions because people would lose the access to the water they can now source for free. The alternative, treated water delivered through closed pipelines, is unaffordable for the poorest part of the population. They would have reverted to hand-dug wells instead, but these are often contaminated.

Any future water plans of covering the Calueque–Oshakati Canal (COC) thus have to be carefully balanced in socio-economic terms. However, the hydrological aspects of loss, as well as potential contributions from different water sources (rivers, floods, and groundwater) have thus far not been investigated in the COC. The effectiveness of any potential measures like the covering of the canal can therefore not be assessed.

The objective of this work was to use spatio-temporal stable isotope patterns to understand controlling processes of canal water quality and quantity as well as influences that potentially endanger the supply of water to the central CEB along the 160 km canal system.

2. Study area

The CEB sedimentary basin extends from the highlands in southern Angola into Northern Central Namibia (Figure 1), covering 165,000 km² [15]. In Northern Namibia, the CEB consists of four major sub-basins called Iishana, Niipele, Olushandja and Tsumeb. Its geological and hydrogeological characteristics were described previously in [18–20]. Perennial tributaries within the Cuvelai catchment are limited to the Angolan part, whereas tributaries in Namibia are generally ephemeral. The topographic gradient is extremely low, with elevations ranging between 1092 and 1110 metres above sea level [21,22]. At a regional scale, drainage is directed towards the saline Etosha Pan, which is the lowest point in the basin. In the CEB region three main aquifers were identified: a shallow, perched aquifer (Kalahari-Ohangwena KOH-0), an upper (KOH-I) and a deep (KOH-II) aquifer.

The majority of the population in the basin lives in rural areas and uses groundwater wells that tap both shallow and deeper aquifers. The COC is supplying the most densely populated area of Namibia with water of the Kunene River. Backup storage is held in the Olushandja reservoir and in water towers at Ogongo, Oshakati and Ondangwa. About 2000 km of pipeline radiate out from purification plants and provide most of the supply for the larger towns. The canal is open along most of its course towards Oshakati, allowing animals and people to freely access the water. During the rainy season, floodwaters regularly fill a multitude of ephemeral streams (locally called oshana or iishana in plural), and wash into the canal, bearing a potential health risk.

The climate of the CEB is characterized as semi-arid with mean annual rainfall ranging from 250 mm/year in the west and up to 550 mm/year in the east. The rainy season lasts

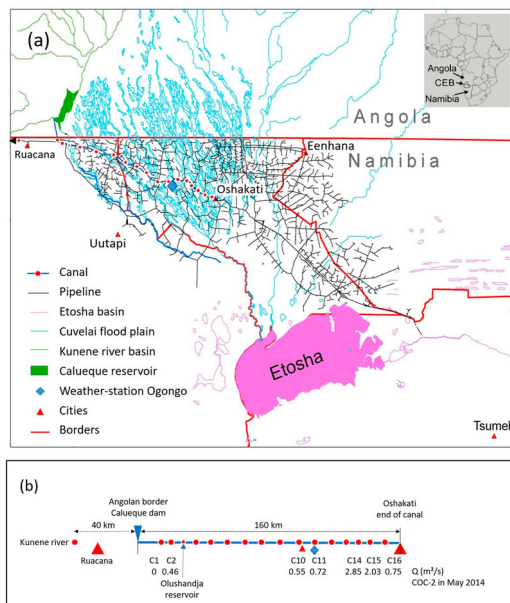


Figure 1. (a) Location of the Cuvelai-Etosha Basin (CEB) in Northern Namibia and sampling sites along the Calueque-Oshakati canal (COC) are indicated as dots; (b) a sketch of the sampling sites (C-1 to C-16) along the canal and measured discharge Q during the COC-2 in May 2014.

from November to April; however, the amount and distribution of rain are quite variable [21]. Mean temperatures range from 17 °C in June and July to 25 °C from October to December. The mean potential evaporation rate can reach up to 3000 mm/year.

Stable isotope studies investigating precipitation patterns in this region have recently been published [23–25], and a local meteoric water line for the Namibian part of the CEB (LMWL-CEB) was defined as $\delta^2\text{H} = 7.20 \times \delta^{18}\text{O} + 4.49$ [24] based on data from eleven stations with 61 samples in total collected and analysed between 2013 and 2016. Unsaturated zone studies involving stable isotopes were conducted to estimate groundwater recharge [26–29]. Stable isotopes and hydrochemistry of the perched aquifer (KOH-0) were described in [21,22] and those of the deep Kalahari-Ohangwena Aquifers (KOH-I and KOH-II) in [19,20].

3. Methods

Water samples were collected from the COC during four field campaigns right before the onset of two consecutive rainy seasons (COC-1: November 2013; COC-3: November 2014), and after the subsequent rainy seasons (COC-2: June 2014; COC-4: May 2015). During each campaign, 16 sites along the canal were sampled. The Kunene River was not accessible close to the canal on the Angolan side behind the border because of visa restrictions. Therefore, water from the Kunene River was sampled at about 40 km distance downstream of the Calueque reservoir on the Namibian side. Samples were also taken at the Olushandja reservoir, but had to be ignored because of missing information on reservoir management; therefore, only 15 points are plotted on the related figures except COC-2, where two extra samples were taken at Oshakati. Temperature (T), electrical conductivity (EC), pH-value and oxygen content were measured *in situ* (Multi 3430, WTW GmbH, Weilheim, Germany). The hydrochemistry of shallow groundwater in the CEB was already described by Hamutoko et al. [21,22].

A maximum abstraction rate of 6 m³/s from the Kunene River at Calueque was agreed between the former colonial regimes Portugal and South Africa (FAO, <http://www.fao.org/3/W7414B/w7414b11.htm>) and followed by Namibian and Angolan authorities; however, to date the intake has been less than the agreed maximum [13,16]. No detailed information on discharge was available for the COC, as water delivery is not steady. Several discharge stations exist, but measurement data held by the responsible authorities are not accessible. Discharge measurements were conducted during COC-2 of the present study on 18 and 19 June 2014 at seven stations along the canal using the velocity area method with a digital flow meter (ADC, Ott Hydromet GmbH, Germany).

The concentrations of major, minor and trace elements were analysed in the laboratory of the German Federal Institute for Geosciences and Natural Resources (BGR) in Hannover. The determination of the concentrations of major and minor ions was done using a Dionex ICS-3000 ion chromatograph (Cl, Br, F, NO₃, NO₂, SO₄). Determination of HCO₃ concentrations was done on a Schott Titroline Alpha Plus automatic titration system according to a modified DIN 38409-H7-2 standard by evaluation of titration curve shapes for the identification and quantitation. Cations were analysed on a Spectro Arcos ICP-OES (Na, K, Ca, Mg, P, Fe, Mn, Al, Si) and a Unicam UV 300 photometer (NH₄).

Aliquots of all samples were analysed for stable isotopes of water (¹⁸O, ¹⁷O and ²H) using a cavity ring-down (CRD) Picarro L2140-i laser analyser equipped with a vaporizer

and autosampler. An additional post-run correction scheme for machine drift was applied [30]. All values are given as δ -values defined by Equation (1):

$$\delta = \left[\frac{R_{SA}}{R_{ST}} - 1 \right] \times 1000, \quad (1)$$

where R_{SA} denotes the isotope ratio of the rare to the more abundant isotope species of a sample and R_{ST} of the standard, respectively. $\delta^{18}\text{O}$ and $\delta^2\text{H}$ values are usually given in per mil (‰) (or mUr) against the international standard Vienna Standard Mean Ocean Water (V-SMOW, normalized to V-SMOW/SLAP scale), and $\delta^{17}\text{O}$ values are given in per mil (‰) or (mUr) against laboratory standards that were calibrated at the Laboratory for Sciences of Climate and Environment (LSCE), France. For notation of δ -values in figures and tables, we follow recommendations given by Brand et al. [31]. Analytical precision of a quality check sample measured in each sequence is better than 0.2 ‰ for $\delta^{18}\text{O}$, 0.8 ‰ for $\delta^2\text{H}$ and 0.05 ‰ for $\delta^{17}\text{O}$ measurements. Deuterium excess (d) values are calculated as $d = \delta^2\text{H} - 8 \times \delta^{18}\text{O}$. ^{17}O excess values ($\Delta^{17}\text{O}$) are given in per meg (10^{-6}) calculated using a regression line after Luz et al. [32]. Here we considered uncertainties for d -values better than 1 ‰ and those of $\Delta^{17}\text{O}$ values better than 20 per meg derived for a quality check sample measured continuously and similar to those given in [33]. High contents of dissolved organic carbon (DOC) can be problematic for laser measurements because of potential interference with the used water absorption bands. Picarro Inc. provides a data correction software called ChemCorrect™ which flags samples with high DOC interference for repetition or discard. This has not shown to be a problem for the samples in this work.

To model the isotopic evolution along the canal, we followed the same approach as Dogramaci et al. [34], who used the following equation by Gibson and Reid [35] to calculate the evaporative water loss from a stream in a dryland area in Australia

$$E / I = \frac{\delta_L - \delta_p}{(\delta^* - \delta_L) \times m}, \quad (2)$$

where E / I is the fraction of evaporation over water inflow, and δ_p and δ_L are the delta values of the in- and outflow along a canal section, respectively. δ^* is the limiting isotope enrichment factor, defined as

$$\delta^* = \frac{h \times \delta_A + \varepsilon}{h - (\varepsilon/1000)}, \quad (3)$$

where h is the relative humidity, δ_A is the delta value of the atmospheric water vapour, and ε is the total fractionation factor, which is the sum of an equilibrium ε^* and a kinetic part ε_K [35]. The value of ε^* for ^2H and ^{18}O follows from the temperature dependent fractionation factors between liquid and vapour (α_{l-v}) by Horita and Wesolowski [36], whereas $\varepsilon_K = (1-h)C_K$, where C_K is the kinetic fractionation constant (14.2 and 12.5 ‰ for ^{18}O and ^2H , respectively). Corresponding values for ^{17}O were derived from the ratio between the natural logarithms of the liquid to vapour fractionation factors, θ :

$$\theta = \frac{\ln(^{17}\alpha_{l-v})}{\ln(^{18}\alpha_{l-v})}, \quad (4)$$

with θ equal to 0.529 for the equilibrium part, and 0.5185 for the kinetic part [10]. Finally,

m is the so-called enrichment slope factor

$$m = \frac{h - (\varepsilon/1000)}{1 - h + (\varepsilon_K/1000)} \quad (5)$$

Values for relative humidity and temperature were obtained from the meteorological station Ogongo (about 100 km west of Oshakati). In the absence of direct measurements of δ_A , it was calculated using isotope equilibrium between atmospheric water vapour and rainfall. For rainfall the following data from Wanke et al. [25] were used: $\delta^2\text{H} = -25.2 \text{ ‰}$ and $\delta^{18}\text{O} = -4 \text{ ‰}$ for COC-1 and COC-3 (November) and $\delta^2\text{H} = -22.6 \text{ ‰}$ and $\delta^{18}\text{O} = -2.3 \text{ ‰}$ for COC-2 and COC-4 (data for May were used, as no data for June were available). Corresponding delta values for ^{17}O in rainfall were derived from $\delta^{17}\text{O} = 0.525 \times \delta^{18}\text{O} + 0.005$ [37] for Windhoek 2013–2014 which is the closest station with ^{17}O records.

4. Results

Weather data reported at the climate station Ogongo (SASSCAL weather net, www.sasscalweathernet.org) in the CEB for the period 2013–2015 and for the sampling campaigns are shown in Figure 2. The austral winter season from May to September is characterized by little to no rainfall, and temperature and humidity are lower than during the summer. Total rainfall for 2014 and 2015 was 111 and 296 mm, respectively. The mean discharge of all measurements during the June 2014 campaign was about 1.05 (± 1) m^3/s . The results of the discharge measurements conducted at the different sites in June 2014 are given in Figure 1(b).

EC values were 58 (± 5) $\mu\text{S}/\text{cm}$ for Kunene River water. Shallow groundwater had EC-values of 144 (± 58) $\mu\text{S}/\text{cm}$ and deeper perched groundwater (KOH-0) 708 (± 177) $\mu\text{S}/\text{cm}$ [21,22]. COC-water was thus less mineralized than the groundwater. The ECs of the COC slightly increased with decreasing distance of the sampling sites to the more populated regions of the CEB. The values for COC-2 behaved differently and did not gradually

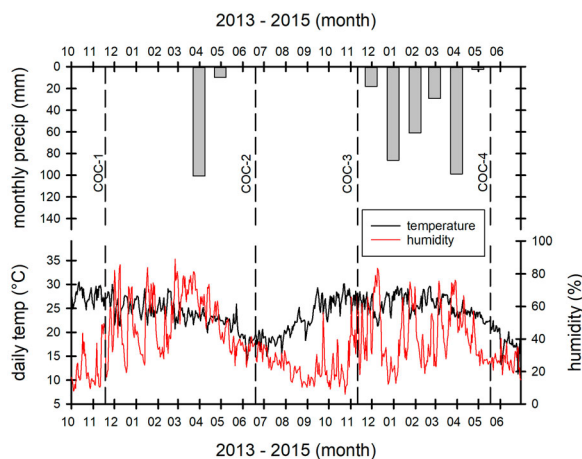


Figure 2. Climate conditions at Ogongo station (www.SASSCALweathernet.org) in the CEB including precipitation, temperature and relative humidity values. Dashed vertical lines indicate the four sampling campaigns (COC-1 to 4).

Table 1. Mean isotope values of samples (*N*) from rain, river water and shallow, perched (KOH-0), and deep (KOH-II) groundwater, collected between 2013 and 2019.

Campaign	<i>N</i>	EC ($\mu\text{S}/\text{cm}$)	$\delta^2\text{H}$ (‰ VSMOW)	$\delta^{18}\text{O}$ (‰ VSMOW)	<i>d</i> (‰ VSMOW)	$\delta^{17}\text{O}$ (‰ VSMOW)	$\Delta^{17}\text{O}$ (per meg)
Rain CEB [24]	61	n.d.	-40.3 ± 36.8	-6.22 ± 5.08	9 ± 6	n.d.	n.d.
Zambesi River ^a	1	n.d.	-17.4	-2.05	-1	n.d.	n.d.
Cuando River ^b	1	37	-12.3	-0.82	-6	-0.338	93
Okavango River ^b	1	35	-30.8	-4.45	5	-2.268	83
Kunene River	4	58 ± 5	-18.4 ± 5.1	-2.53 ± 1.07	2 ± 4	-1.253 ± 0.555	82 ± 20
COC-all	62	52 ± 18	-16.4 ± 4.6	-2.11 ± 0.98	0 ± 3	-0.932 ± 0.518	81 ± 12
Shallow GW [21]	9	144 ± 58	-35.8 ± 5.6	-4.53 ± 1.17	0 ± 4	n.d.	n.d.
KOH-0 [21]	14	708 ± 177	-51.6 ± 3.9	-7.28 ± 0.63	7 ± 2	n.d.	n.d.
KOH-II [18] ^c	10	932 ± 338	-65.9 ± 1.0	-9.52 ± 0.11	10 ± 1	n.d.	n.d.

Sampled: ^aOct. 2013, ^bJune 2015, ^cMarch 2019, n.d. not determined.

increase. Tables 1 and 2 show mean EC values and standard deviations for rivers, groundwater and canal water collected in the CEB for comparison. Figure 3 shows the basic hydrochemical data of groundwater and samples from the COC in a Piper diagram. The COC water, which directly reflects the chemical composition of Kunene water, can be characterized as a mixed type, $\text{Ca}^{2+}\text{-Mg}^{2+}\text{-Na}^+\text{-K}^+\text{-HCO}_3^-$. While bicarbonate is the dominating anion for all groundwater samples, some show a development towards chloride and sulfate water types. On the cation side, in general, deep groundwater is characterized by Na, perched aquifers by Ca–Mg, with some variations and overlaps. In a more extended study, Hamutoko et al. [21,22] managed to distinguish three water types for shallow perched groundwater (KOH-0): $\text{Na}^+\text{-K}^+\text{-HCO}_3^-$ or $\text{Ca}^{2+}\text{-Mg}^{2+}\text{-HCO}_3^-$ as dominant ions, or a mixed water type. Deeper perched groundwater (KOH-0) was classified as $\text{Ca}^{2+}\text{-Mg}^{2+}\text{-HCO}_3^-$ and $\text{Na}^+\text{-K}^+\text{-HCO}_3^-$ water and also $\text{Na}^+\text{-K}^+\text{-HCO}_3^-$ for KOH-I [22]. $\text{Na}^+\text{-K}^+\text{-HCO}_3^-$ is also the water type of the deep Ohangwena aquifer (KOH-II) (Figure 3).

A compilation of mean stable isotope values of the most important water sources in the region is shown in Table 1. The mean values for the COC-campaigns are listed in Table 2. Stable isotope values of rivers (Kunene, Okavango, Cuando and Zambesi), and groundwater (shallow and perched groundwater KOH-0, and deep KOH-II) as well as values for all four COC-campaigns are plotted in Figure 4. The global meteoric water line and the local meteoric water line for the CEB (LMWL-CEB after [24]) (thin and bold lines in Figure 4) are included for comparison. Groundwater samples from shallow,

Table 2. Summary on field campaigns conducted along the Calueque-Oshakati canal (COC), including information on collected samples (*N*), cumulated precipitation (*P*) prior to each sampling campaign, mean and standard deviation of electrical conductivity (EC), and stable isotope values.

Campaign	Date	<i>N</i>	<i>P</i> (mm)	EC ($\mu\text{S}/\text{cm}$)	$\delta^2\text{H}$ (‰ VSMOW)	$\delta^{18}\text{O}$ (‰ VSMOW)	<i>d</i> (‰ VSMOW)	$\delta^{17}\text{O}$ (‰ VSMOW)	$\Delta^{17}\text{O}$ (per meg)
COC-1	17–19 Nov. 2013	15	0	53 ± 8	-10.32 ± 2.0	-0.77 ± 0.5	-4 ± 2	-0.331 ± 0.263	77 ± 8
COC-2	16–21 Jun. 2014	17 ^a	111	64 ± 32	-21.25 ± 2.1	-3.03 ± 0.38	3 ± 1	-1.513 ± 0.202	91 ± 9
COC-3	11–12 Nov. 2014	15	0	45 ± 6	-15.0 ± 2.3	-1.83 ± 0.56	0 ± 2	-0.881 ± 0.295	84 ± 7
COC-4	11–13 May 2015	15	296	47 ± 11	-18.3 ± 1.5	-2.68 ± 0.37	3 ± 1	-1.346 ± 0.193	69 ± 13

^aTwo samples extra taken at Oshakati.

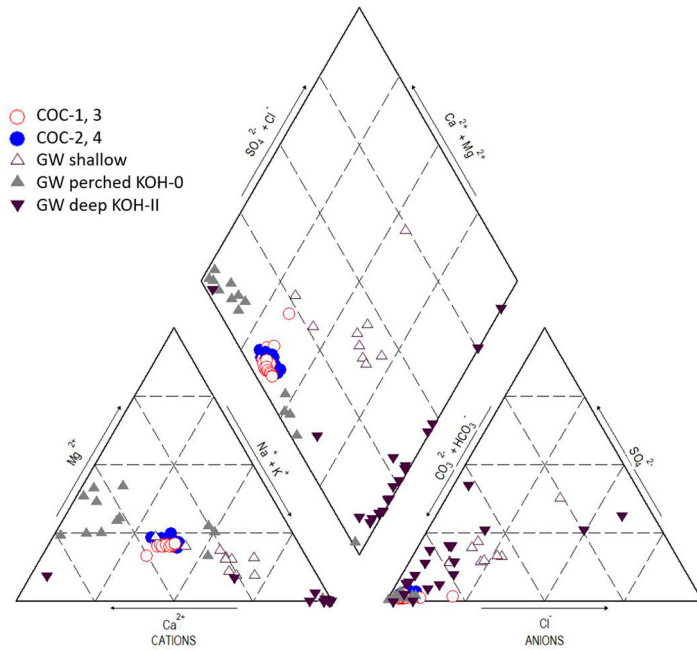


Figure 3. Piper plot indicating hydrochemical patterns of COC samples collected during four sampling campaigns, as well as shallow and deeper (KOH-0) groundwater (after [21]) and from 200 m deep Ohangwena (KOH-II) aquifer.

perched and deeper KOH-I aquifers in the CEB show distinct clusters for shallow and deep groundwater as was described earlier [18,20]. All groundwater samples seem to plot below the LMWL-CEB.

The data points for all four COC-sampling campaigns plot on an evaporation line ($\delta^2\text{H} = 4.62 \delta^{18}\text{O} - 7.19$; $R^2 = 0.99$) that also characterizes evaporation from the iishana (Figure 4

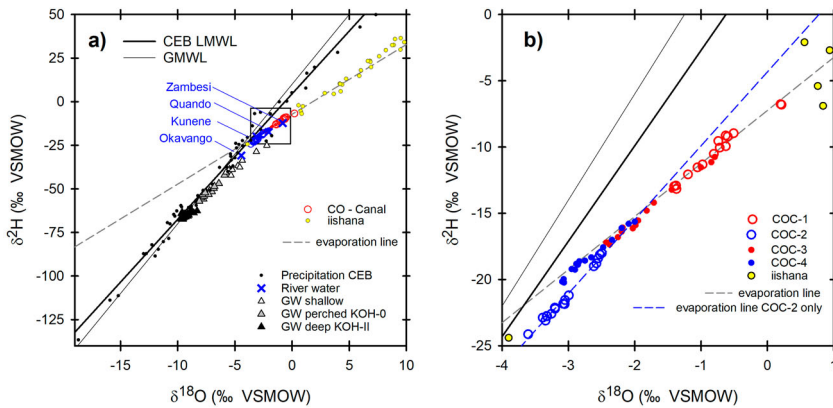


Figure 4. $\delta^2\text{H}$ vs. $\delta^{18}\text{O}$ plot of (a) of precipitation, groundwater and surface water; b) canal water COC-1 to 4 collected during the four field campaigns (LMWL-CEB is drawn after [24]; iishana samples are after [25]).

(a). In Figure 4(b) the data points of COC-1, COC-3 and COC-4 plot on a similar evaporation line, whereas the points for COC-2 plot along a different trajectory ($\delta^2\text{H} = 5.58 \delta^{18}\text{O} - 4.34$; $R^2 = 0.99$). Pre-rainy season values (November – in red symbols) are more enriched than post-rainy season values (May, June – in blue symbols). Almost all isotope values of the samples that were collected from flooded iishana after the rainy season in May 2014 (yellow symbols in Figure 4, described in [24]) are more enriched than canal water from the COC campaigns.

The spatial distribution of EC, $\delta^2\text{H}$, d -values and $\delta^{17}\text{O}$ is presented in Figure 5, by plotting the data versus distance to the Angolan border, from where Kunene River water (source water) is delivered. A gradual rise of EC and $\delta^2\text{H}$ and $\delta^{17}\text{O}$ values with distance is visible for three out of four campaigns. The d -values (Figure 5(c)) for the same three

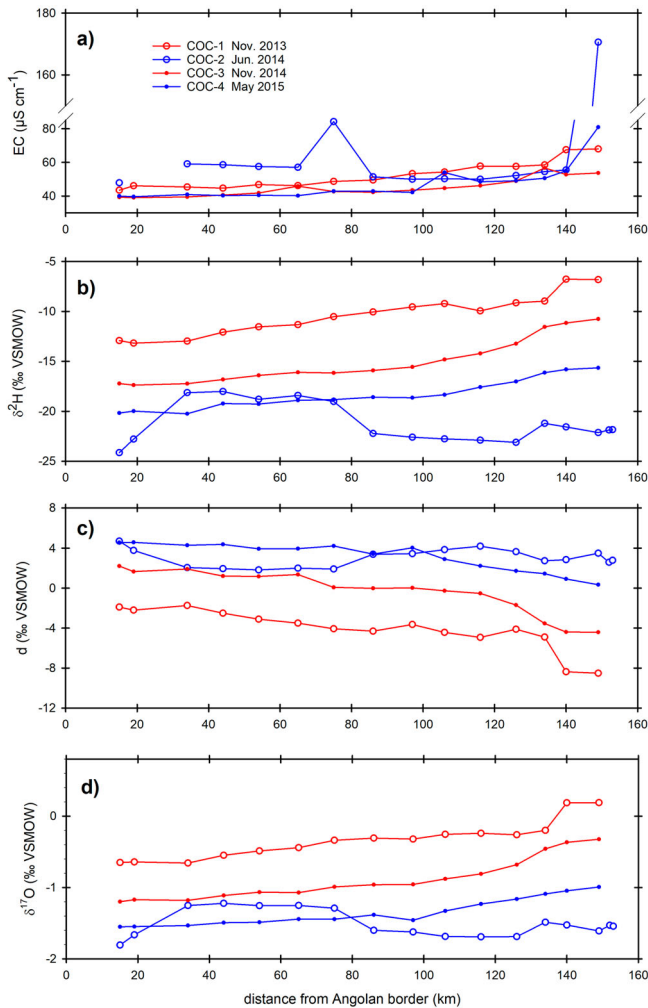


Figure 5. (a) EC, (b) $\delta^2\text{H}$ values, (c) d -values and, (d) $\delta^{17}\text{O}$ values shown against flow distance (km) from the Angolan border.

campaigns become more negative with increasing distance from the source, which is more pronounced during the warm pre-rainy season (red symbols).

5. Discussion

The values for the KOH-II aquifer plot on the LMWL-CEB, which was most likely recharged during colder time periods and/or at higher elevations in the Angolan mountain range in the Northern part of the CEB [38]. Mean d -values of Kunene, COC and shallow groundwater are relatively close, but quite variable between the four campaigns. The $\Delta^{17}\text{O}$ values of the different components shown in Table 1 (between 80 and 90 per meg) are in the same range, when uncertainty of the measurements is considered.

The samples taken during the COC-2 campaign show a different pattern than those of the other campaigns. The samples of the COC-2 campaign (Figure 5(b,c)) seem to be more enriched for the first seven stations and d -values indicate more evaporation for these stations. For the rest of the stations, the $\delta^2\text{H}$ values are more negative. The values for COC-2 plot along an evaporation line in the $\delta^2\text{H}$ vs. $\delta^{18}\text{O}$ plots that deviates from the evaporation line of the other campaigns (Figures 4 and 6(a–d)). $\delta^{17}\text{O}$ values for COC-2 seem to be consistent with the other campaigns though (Figure 6(e–h)). The discharge measurements conducted during COC-2 showed high discharge ($> 2 \text{ m}^3/\text{s}$) at the end of the canal (stations C14, C15) and almost no flow at C1 (Figure 1(b)). An explanation for this unexpected pattern could be that during this time water from the Olushandja reservoir, which at that time of the year is a mixture of Kunene water and to a lesser amount iishana water, was used to backup the canal water. No details on reservoir management were available to test this hypothesis.

The lines in Figure 6 represent the relationship between the isotope δ -values according to the Craig–Gordon model (Equations (2)–(5)), and the values indicate progressive fractions of water loss. The evaporative loss that was estimated by $\delta^2\text{H}$ vs. $\delta^{18}\text{O}$ and $\delta^{17}\text{O}$ vs. $\delta^{18}\text{O}$ produce about the same results for each campaign despite the fact that data on $\delta^{17}\text{O}$ vs. $\delta^{18}\text{O}$ diagram fit well to the calculated evaporation lines, whereas data on the $\delta^2\text{H}$ vs. $\delta^{18}\text{O}$ diagrams are frequently above the calculated evaporation line.

The results indicate that up to 10 % of canal water was lost by evaporation at the end of the dry season (COC-1 and COC-3) and up to 5 % after the rainy season (COC-4). Assuming a uniform evaporation rate, the evaporated fraction would increase linearly along the 160 km of flow length, resulting in an average fraction of $(10 \% + 0) / 2 = 5 \%$ after the dry season (or 2.5 % after the wet season). The water volume is about $160,000 \text{ m}^3$ in the canal (160 km flow length, 2.5 m canal width and 0.4 m water depth), so an overall water loss of circa 8000 m^3 is estimated (equal to $20 \text{ L}/\text{m}^2$ evaporation loss). These evaporative losses are on the same order as those found by Dogramaci et al. [34] for a dryland stream in northwestern Australia (up to $\sim 4 \%$), but somewhat lower than the 2–32 % range reported by Kong et al. [39] for irrigation canals in the North China Plain.

Chloride concentrations are expected to increase during evaporation and have been used in other studies to quantify evaporation losses (e.g. Dogramaci et al. [34]). The measured chloride concentrations, however, do not show a systematic increase with distance along the canal, but display a somewhat erratic pattern instead (not shown). Given the relatively low evaporation rates ($< 10 \%$), the resulting increase of the chloride

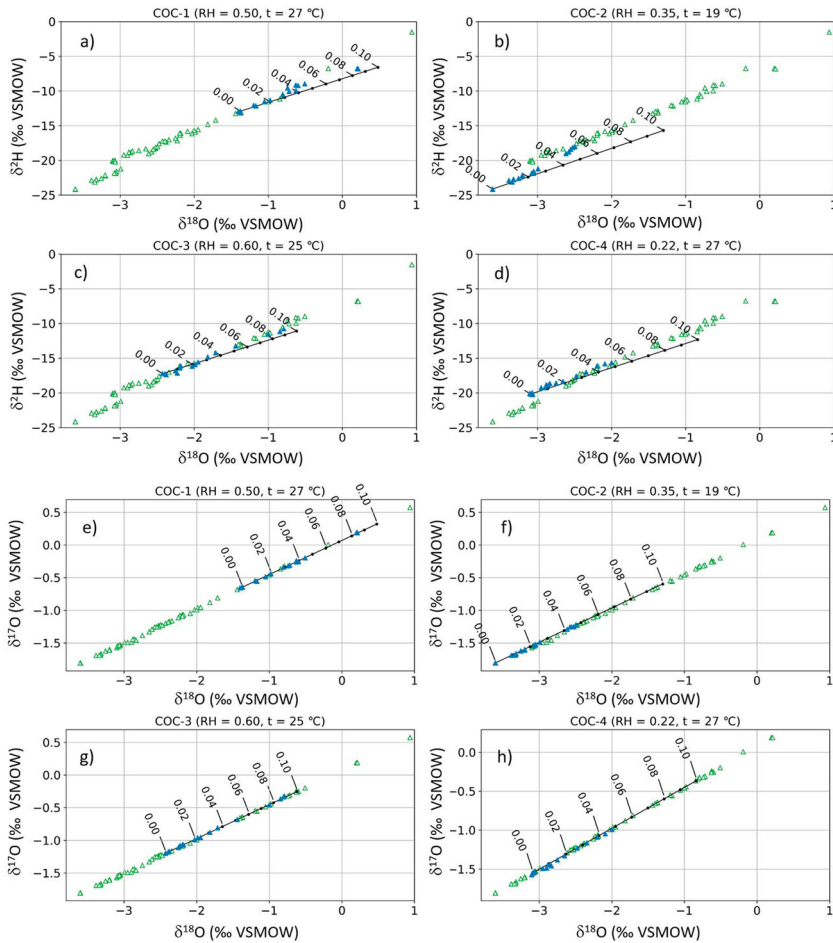


Figure 6. Modelled evaporation loss correlated with $\delta^2\text{H}$ and $\delta^{18}\text{O}$ values for (a) COC-1 campaign in November 2013, (b) COC-2 campaign in June 2014, (c) COC-3 campaign in November 2014 and (d) COC-4 campaign in May 2015 (upper part a–d) and from $\delta^{17}\text{O}$ and $\delta^{18}\text{O}$ values (lower part e–h). Relative fractions of water loss from the canal by evaporation are indicated by numbers and samples from all campaigns are plotted in open symbols for comparison to those from the actual campaign in filled symbols.

concentration is close to the analytical precision, and may therefore not be clearly visible in the data. Moreover, the chloride concentrations are < 1 mg/L and are therefore sensitive to contamination by external sources, including anthropogenic pollution but also atmospheric dust. This demonstrates the superiority of stable water isotopes over chloride to quantify evaporation in this environment.

An estimated up to 10 % loss is relatively small compared to what is potentially lost from a piped network (known from other countries) [40]. While from this result the canal appears as a well-performing water distribution infrastructure, it also has to be considered that we have not investigated other factors that influence the water quality in this open canal, e.g. inflow of contaminated surface water and recommend further investigations.

6. Conclusion

Isotope and hydrochemical evolution of canal water which is distributed from the Kunene River was compared to local rain, Kunene source water and available groundwater in the region. Hydrochemistry and progressive loss of water reflect a system vulnerability due to uncovered canal and pollution risks. Canal water displays stable isotope enrichment in three out of four campaigns, from which an evaporative loss of water of up to 10 % was inferred. Three of the four campaigns showed progressive enrichment along the canal, as would be expected when the inlet water is flowing at a uniform rate. During the COC-2 campaign, however, the enrichment pattern along the canal was not consistent with this model, and discharge measurements indicated more complex flow conditions. Thus, while isotope techniques by themselves can already provide valuable clues about hydrological processes and quantitative estimates of evaporation, independent verification by discharge measurements remains necessary. The lack of information about the operational management of the canal infrastructure also formed an impediment during this study. These challenges highlight the need for multi-method investigations, but it is clear that isotopes can play a key role in these.

Acknowledgements

The authors gratefully acknowledge the contributions by Shoopala Uugulu and Wilhelm Nuumbembe from University of Namibia, as well as Martin Quinger, Christoph Lohe, Markus Wallner and Falk Lindenmaier at BGR, for their help during fieldwork and with all logistics. We would like to thank Dr István Fórizs and an anonymous reviewer for all comments and corrections to improve this manuscript.

Disclosure statement

No potential conflict of interest was reported by the authors.

Funding

We would like to acknowledge financial support by the Bundesministerium für Bildung und Forschung (BMBF) within the SASSCAL project (South African Science and Service Center for Climate Change, Agriculture and Landuse) under contract number 01LG1201L (www.sasscal.org).

ORCID

Paul Koeniger  <http://orcid.org/0000-0002-1197-6274>

References

- [1] Craig H, Gordon LI. Deuterium and oxygen 18 variations in the ocean and the marine atmosphere. In: Tongiorgi E, editor. *Stable isotopes in oceanographic studies and paleotemperatures*. Pisa: Laboratorio di Geologia Nucleare; 1965. p. 9–130.
- [2] Skrzypek G, Mydlowski A, Dogramaci S, et al. Estimation of evaporative loss based on the stable isotope composition of water using hydrocalculator. *J Hydrol*. 2015;523:781–789.
- [3] Kebede S, Travi Y, Rozanski K. The $\delta^{18}\text{O}$ and $\delta^2\text{H}$ enrichment of Ethiopian lakes. *J Hydrol*. 2009;365(3):173–182.

- [4] Strauch G, Oyarzun J, Fiebig-Wittmaack M, et al. Contributions of the different water sources to the Elqui river runoff (northern Chile) evaluated by H/O isotopes. *Isot Environ Health Stud.* 2006;42:303–322.
- [5] Koeniger P, Leibundgut C, Stichler W. Spatial and temporal characterization of stable isotopes in river water as indicators of groundwater contribution and confirmation of modelling results; a study of the Weser river, Germany. *Isot Environ Health Stud.* 2009;45(4):289–302.
- [6] Gibson JJ, Aggarwal PK, Hogan J, et al. Isotope studies in large river basins: a new global research focus. *Eos Trans AGU.* 2002;83(52):613–617.
- [7] Aggarwal PK, Alduchov O, Araguas Araguas L, et al. New capabilities for studies using isotopes in the water cycle. *Eos Trans AGU.* 2007;88(49):537–538.
- [8] Vitvar T, Aggarwal PK, Herczeg AL. Global network is launched to monitor isotopes in rivers. *Eos Trans AGU.* 2007;88(33):324–326.
- [9] Farquhar GD, Hubick KT, Condon AG, et al. Carbon isotope fractionation and plant water-use efficiency. In: Rundel PW, Ehleringer JR, Nagy KA, editors. *Stable isotopes in ecological research.* New York (NY): Springer; 1989. p. 21–40.
- [10] Surma J, Assonov S, Herwartz D, et al. The evolution of ^{17}O -excess in surface water of the arid environment during recharge and evaporation. *Sci Rep.* 2018;8:4972.
- [11] Kluge T, Liehr S, Lux A, et al. IWRM concept for the Cuvelai Basin in northern Namibia. *Phys Chem Earth.* 2008;33(1–2):48–55.
- [12] Niemann S. Indigenous water resources management and water utilisation in Northern Namibia (former 'Ovamboland') – can tradition help to overcome current problems? *Erde.* 2002;133:183–199.
- [13] Luetkemeyer R, Stein L, Drees L, et al. Blended drought index: integrated drought hazard assessment in the Cuvelai-Basin. *Climate.* 2017;5(3):51.
- [14] Faulstich L, Schulte A, Arendt R, et al. Water quality of intensely used surface water bodies in the Cuvelai Basin (Northern Namibia) at the end of the dry season 2017. In: Chiffard P, Karthe D, Möller S, editors. *Beiträge zum 49. Jahrestreffen des Arbeitskreises Hydrologie vom 23.–25. November 2017 in Göttingen.* Augsburg: Institut für Geographie; 2018. p. 9–21. (*Geographica Augustana*; 26).
- [15] Miller RMG, Pickford M, Senut B. The geology, paleontology and evolution of the Etosha Pan, Namibia: implications for terminal Kalahari deposition. *S Afr J Geol.* 2010;113:307–334.
- [16] Directorate of Rural Water Supply. 10 years: Directorate of Rural Water Supply, 1993–2003. Windhoek, Namibia: Ministry of Agriculture, Water and Rural Development; 2004. (*Namibia Water Resources Management Review*).
- [17] Mendelson J, Jarvis A, Robertson T. A profile and Atlas of the Cuvelai-Etosha basin. Windhoek: Ministry of Agriculture, Water and Rural Development; 2013.
- [18] Christelis G, Struckmeier W, editors. *Groundwater in Namibia – an explanation to the hydrogeological map.* Windhoek: Department of Water Affairs, Ministry of Agriculture, Water and Rural Development; 2001.
- [19] Lindenmaier F, Miller R, Fenner J, et al. Structure and genesis of the Cubango Megafan in northern Namibia: implications for its hydrogeology. *Hydrogeol J.* 2014;22:1431–2174.
- [20] Himmelsbach T, Beyer M, Wallner M, et al. Deep, semi-fossil aquifers in Southern Africa: a synthesis of hydrogeological investigations in northern Namibia. In: Revermann R, Krewenka KM, Schmiedel U, et al., editors. *Climate change and adaptive land management in Southern Africa - assessments, changes, challenges, and solutions.* Göttingen: Klaus Hess Publishers; 2018. p. 66–74. (*Biodiversity & Ecology*; 6).
- [21] Hamutoko J, Wanke H, Koeniger P, et al. Hydrochemical and isotope hydrological characterisation of perched aquifers in the Cuvelai-Etosha Basin, Namibia. *Isot Environ Health Stud.* 2017;53(4):382–399.
- [22] Hamutoko JT, Post VEA, Wanke H, et al. The role of local perched aquifers in regional groundwater recharge in semi-arid environments: evidence from the Cuvelai-Etosha Basin, Namibia. *Hydrogeol J.* 2019;27:2399–2413.
- [23] Kaseke KF, Wang L, Wanke H, et al. An analysis of precipitation isotope distributions across Namibia using historical data. *PLoS ONE.* 2016;11(5):e0154598.

- [24] Wanke H, Gaj M, Beyer M, et al. Comparison of stable isotope characteristics in the Cuvelai-Etosha Basin, Namibia with local meteoric water patterns of Southern Africa. *Isot Environ Health Stud.* 2018;54(6):588–607.
- [25] Wanke H, Beyer M, Hipondoka M, et al. The long road to sustainability: integrated water quality and quantity assessments in the Cuvelai-Etosha Basin, Namibia. In: Revermann R, Krewenka KM, Schmiedel U, et al., editors. *Climate change and adaptive land management in Southern Africa – assessments, changes, challenges, and solutions.* Göttingen: Klaus Hess Publishers; 2018. p. 75–83. (Biodiversity & Ecology; 6).
- [26] Beyer M, Gaj M, Hamutoko J, et al. Estimation of groundwater recharge via deuterium labeling in the semi-arid Cuvelai-Etosha Basin, Namibia. *Isot Environ Health Stud.* 2015;51(4):533–552.
- [27] Beyer M, Koeniger P, Gaj M, et al. A deuterium-based labeling technique for the investigation of rooting depths, water uptake dynamics and unsaturated zone water transport in semiarid environments. *J Hydrol.* 2015;533:627–643.
- [28] Gaj M, Beyer M, Koeniger P, et al. In situ unsaturated zone water stable isotope (^2H and ^{18}O) measurements in semi-arid environments: a soil water balance. *Hydrol Earth Syst Sci.* 2016;20(2):715–731.
- [29] Gaj M, Kaufhold S, Koeniger P, et al. Mineral mediated isotope fractionation of soil water. *Rapid Commun Mass Spectrom.* 2016;31:269–280.
- [30] Van Geldern R, Barth JAC. Optimization of instrument setup and post-run corrections for oxygen and hydrogen stable isotope measurements of water by isotope ratio infrared spectroscopy (IRIS). *Limnol Oceanogr Meth.* 2012;10:1024–1036.
- [31] Brand WA, Coplen TB. Stable isotope deltas: tiny, yet robust signatures in nature. *Isot Environ Health Stud.* 2012; 48(3):393–409.
- [32] Luz B, Barkan E. Variations of $^{17}\text{O}/^{16}\text{O}$ and $^{18}\text{O}/^{16}\text{O}$ in meteoric waters. *Geochim Cosmochim Acta.* 2010;74:6276–6286.
- [33] Pierchala A, Rozanski K, Dulinski M, et al. High-precision measurements of $\delta^2\text{H}$, $\delta^{18}\text{O}$ and $\delta^{17}\text{O}$ in water with the aid of cavity ring-down laser spectroscopy. *Isot Environ Health Stud.* 2019;55(3):290–307.
- [34] Dogramaci S, Skrzypek G, Dodson W, et al. Stable isotope and hydrochemical evolution of groundwater in the semi-arid Hamersley Basin of subtropical northwest Australia. *J Hydrol.* 2012;475:281–293.
- [35] Gibson JJ, Reid R. Stable isotope fingerprint of open-water evaporation losses and effective drainage area fluctuations in a subarctic shield watershed. *J Hydrol.* 2010;381(1–2):142–150.
- [36] Horita J, Wesolowski DJ. Liquid–vapor fractionation of oxygen and hydrogen isotopes of water from the freezing to the critical temperature. *Geochim Cosmochim Acta.* 1994;58(16):3425–3437.
- [37] Kaseke KF, Wang L, Wanke H, et al. Precipitation origins and key drivers of precipitation isotope (^{18}O , ^2H , and ^{17}O) compositions over Windhoek. *J Geophys Res Atmos.* 2018;123:7311–7330.
- [38] Wallner M, Houben G, Lohe C, et al. Inverse modeling and uncertainty analysis of potential groundwater recharge to the confined semi-fossil Ohangwena II aquifer, Namibia. *Hydrogeol J.* 2017;25(8):2303–2321.
- [39] Kong X, Wang S, Liu B, et al. Impact of water transfer on interaction between surface water and groundwater in the lowland area of North China Plain. *Hydrol Process.* 2018;32:2044–2057.
- [40] Burn LS, De Silva D, Eiswirth M, et al. Pipe leakage – future challenges and solutions. *Pipes Wagga Wagga Conference 1999, 12–14 October, Wagga Wagga, Australia.*